Analysis of molecular ligand functionalization process in nano-molecular electronic devices containing densely packed nano-particle functionalization shells

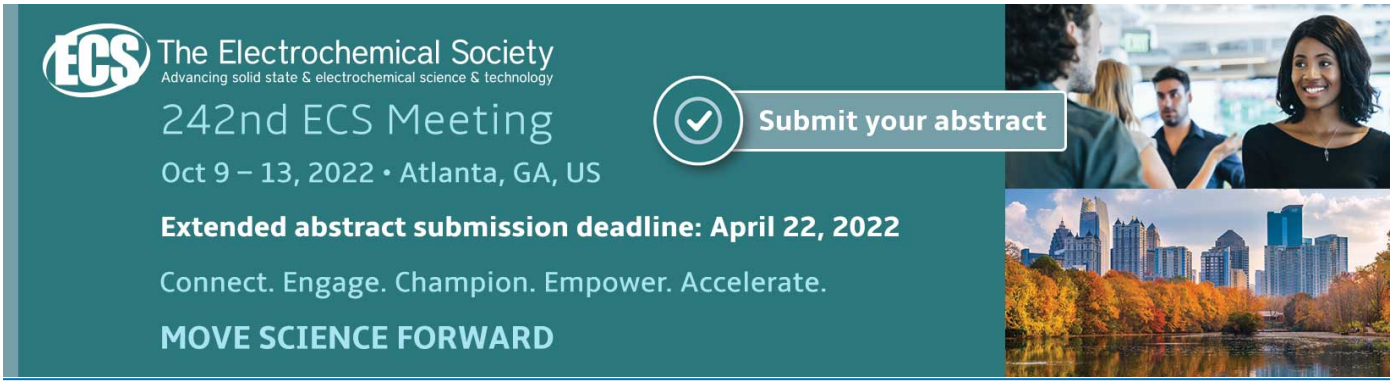

OPEN ACCESS
IOP Publishing
Nanotechnology

Nanotechnology **33** (2022) 255706 (8pp)
https://doi.org/10.1088/1361-6528/ac5cfc

Analysis of molecular ligand functionalization process in nano-molecular electronic devices containing densely packed nano-particle functionalization shells

Omer Sher[1,2], Yuanyuan Han[1], Haoyuan Xu[1,3], Hu Li[1,4], Tianbo Daun[1], Sharath Kumar[1], Anton Grigoriev[5], Pritam Kumar Panda[5], Andreas Orthaber[6], Francoise Serein-Spirau[7], Thibaut Jarrosson[7], S Hassan M Jafri[1,2] and Klaus Leifer[1,*]

[1] Applied Materials Science, Department of Engineering Sciences, Uppsala University, PO Box 534, Uppsala SE-75121, Sweden
[2] Department of Electrical Engineering, Mirpur University of Science and Technology, Mirpur Azad Jammu and Kashmir 10250, Pakistan
[3] School of Metallurgy, Northeastern University, Shenyang City, 110819, People's Republic of China
[4] Shandong Technology Centre of Nanodevices and Integration, School of Microelectronics, Shandong University, Jinan 250101, People's Republic of China
[5] Condensed Matter Theory, Department of Physics and Astronomy, Uppsala University, PO Box 516, Uppsala SE-75120, Sweden
[6] Department of Chemistry, Ångström Laboratory, Uppsala University, PO Box 523, Uppsala SE-75120, Sweden
[7] Université de Montpellier, Institut Charles Gerhardt de Montpellier, UMR CNRS 5253, Ecole Nationale Supérieure de Chimie de Montpellier, 1919 route de Mende, F-34000 Montpellier, France

E-mail: Hassan.Jafri@must.edu.pk and Klaus.Leifer@angstrom.uu.se

Received 15 October 2021, revised 20 February 2022
Accepted for publication 11 March 2022
Published 1 April 2022

Abstract

Molecular electronic devices based on few and single-molecules have the advantage that the electronic signature of the device is directly dependent on the electronic structure of the molecules as well as of the electrode-molecule junction. In this work, we use a two-step approach to synthesise functionalized nanomolecular electronic devices (nanoMoED). In first step we apply an organic solvent-based gold nanoparticle (AuNP) synthesis method to form either a 1-dodecanethiol or a mixed 1-dodecanethiol/ω-tetraphenyl ether substituted 1-dodecanethiol ligand shell. The functionalization of these AuNPs is tuned in a second step by a ligand functionalization process where biphenyldithiol (BPDT) molecules are introduced as bridging ligands into the shell of the AuNPs. From subsequent structural analysis and electrical measurements, we could observe a successful molecular functionalization in nanoMoED devices as well as we could deduce that differences in electrical properties between two different device types are related to the differences in the molecular functionalization process for the two different AuNPs synthesized in first step. The same devices yielded successful NO_2 gas sensing. This opens the pathway for a simplified synthesis/fabrication of molecular electronic devices with application potential.

* Author to whom any correspondence should be addressed.

Supplementary material for this article is available online

Keywords: nanoparticle-nanoelectrode platform, molecular electronic devices, organic molecules, gas sensing, functionalization process

(Some figures may appear in colour only in the online journal)

Introduction

The impact of the field of few and single-molecule electronics is largely due to the exciting possibility to relate electrical measurements on one or few molecules directly to their structure and electronic properties. Sophisticated experimental setups at laboratory scale [1] were built based on scanning tunnelling microscope break junctions, mechanically controlled break-junctions [2, 3] and conductive atomic force microscopy (C-AFM) [1, 4, 5]. The molecular junctions in such two terminal devices were shown to act as switches [6], diodes [7, 8], sensors [9], and transistors [10–12].

Though, to our knowledge, the field still has difficulties [13] to make the step from laboratory setups and experiments into applications. One of the difficulties is that in single molecule devices, apart from their mostly bulky experimental setup, the nanometer spaced electrodes can change their shape in the nanometer range [14]. Using a molecular electronics platform where molecule functionalized AuNPs are placed between nanoelectrodes, so-called nanoMoED devices, applications seem to be in reach [9, 15]. Such nanoMoED devices have the advantage of being portable, long term stable as well as they can be operated at standard conditions [14].

The use of standard cleanroom techniques for the structuring of such devices allows for their large-scale fabrication. Nanoelectrodes prepared by electrodeposition, nanolithography and focused ion beam (FIB) techniques at a length scale of few 10 nm are suitable candidates to fabricate nanoMoED devices with specific functions for application purposes [16–20]. In this case, the nanogap spacing is a multiple of the length of most molecules used in molecular electronics and the gap is therefore bridged using AuNPs functionalized with ligand molecules. An advantage of this device geometry with larger electrode spacing as compared to break junctions is that small changes of electrode morphology will not impact the device performance [14].

A key to the fabrication of such nanoMoED devices is the synthesis of the nanoparticles, AuNPs in this work. Ideally, the AuNPs should be synthesised directly with the ligand shell containing the molecules, which are responsible for the functionality of a nanoMoED device. Though very often, the most important result of the synthesis process is to obtain AuNPs of a certain size and with a similar size distribution. Very often, this goal cannot be achieved by adding the required functionalizing molecule in the synthesis step; in the worst case the AuNPs will agglomerate or not form at all. Therefore, the AuNP synthesis process and the functionalization step should be ideally separated.

In fact, it is possible to separate AuNP synthesis and functionalization by applying a ligand functionalization process after the synthesis process of AuNPs [21–23], where single up to a few molecules with tailored properties are placed in the AuNPs ligand shell by molecular functionalization [24, 25].

In a previous published work, we showed successful ligand functionalization experiments in nanoMoED devices that contained AuNPs with a ligand shell composed of a mixture of α, ω alkanedithiol and α,ω alkanedithiol molecules containing a trityl molecule as endgroup [26, 27]. High device reproducibility and long-term stability have been reached [23, 26, 28, 29]. However, there is nearly no possibility to modify the primary functionalization shell of these AuNPs, i.e. the ligand shell that the AuNPs have after synthesis.

In order to obtain a more flexible primary ligand coating of the AuNPs, a synthesis scheme containing a mixture of alkanethiol molecules and ω-tetraphenylmethane functionalized alkane thiols was developed which facilitated further molecular functionalization in nanoMoED devices [22].

Here, we use this straight-forward synthesis method to successfully prepare AuNPs with long-chain alkane-monothiols such as 1-dodecanethiol and present a study of ligand functionalization in the nanoMoED platform using two primary functionalization shells. We thus overcome the issue of synthesis of special molecules during nanoparticle formation as well as we can use a tuneable primary NP functionalization shell. We compare ligand functionalization results carried out on 1-dodecanethiol coated AuNPs and on AuNPs which have a mixed functionalization shell consisting of 1-dodecanethiol together with a 1-dodecanethiol molecule terminated by a bulky end group of tris-[(para-tert-butyl) phenyl] methyl phenyl. The electrical resistance of the nanoMoED containing the two types of functionalized AuNPs devices was evaluated. The structures of the functionalized AuNPs were analysed by using scanning electron microscope (SEM), transmission electron microscope (TEM), dynamic light scattering (DLS), and thermogravimetric (TGA) analysis. The differences in the low bias electrical resistance of devices were related to differences in the functionalization shell of the AuNPs. Gas sensing measurements were carried out on nanoMoED devices functionalized with biphenyl-4,4-dithiol molecules. Thus, we obtain a viable route to prepare nano-sized nanoMoED devices based on hybrid materials.

Methods and materials

Chemicals and materials

Gold (III) chloride hydrate (∼50% Au basis), 1-dodecanethiol (⩾98%), triethylamine (⩾99.5%), biphenyl-4,4-dithiol (BPDT, 95%), tetrahydrofuran (⩾99.9%), ethanol (99%) and toluene (anhydrous, ⩾99.8%) were purchased from the Sigma-Aldrich. The molecule ω-tetraphenyl ether substituted

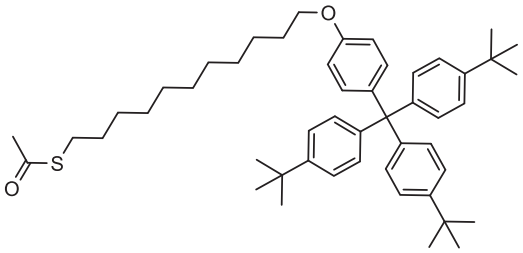

FC196
Chemical Formula: $C_{50}H_{68}O_2S$
Molecular Weight: 733,152

Figure 1. The molecule ω-tetraphenyl ether substituted 1-dodecanethiol called as stopper molecule.

1-dodecanethiol, which is called stopper molecule in this article, was synthesized as described in Calard *et al* [22].

Synthesis of thiolate-capped gold nanoparticles

Two types of thiolate-capped AuNPs were synthesized in this experimental work, including 1-dodecanethiol capped AuNPs (DDT-AuNP) and AuNPs capped by a mixed ligand shell consisting of stopper molecules plus 1-dodecanethiol molecules (St-AuNP). The AuNPs were prepared using a mild and efficient single-organic-phase method [30]. Briefly, for the synthesis of AuNPs of type 1, $HAuCl_4{\cdot}3H_2O$ (40 mg 0.1 mmol) was dissolved in THF (10 ml) and this solution was subsequently mixed with 1-dodecanethiol (0.1 mmol) by stirring vigorously for 15 min until it turned into cloudy form. Then, the reducing agent triethylsilane (0.1 mmol) was introduced in the solution drop-wise. After stirring over 6 h, the NPs solution was filtered to remove big size particles using micro-pore size filter paper, ethanol was added to precipitate the AuNPs. The collected AuNPs were dispersed in toluene uniformly (1 mg ml^{-1}) for the molecular functionalization reaction described below. The synthesis of type-2 AuNPs is identical with the difference that a mixture of 1-dodecanethiol and stopper molecules (95:5 mole ratio, 0.1 mmol in total) are added to the HAuCl4·3H2O solution in THF. The chemical structure of stopper molecule is given in the figure 1.

Fabrication of nanoMoED platform and electrical characterization

The fabrication of nanoelectrode setup is described in detail in [19, 20]. In brief, in the first step, electron beam lithography is used to fabricate nanowires of Au as well as 200 micron large contacts. Then, a focussed ion beam with a Gallium (Ga^+) ion source, is used at an acceleration voltage of 30 kV to sputter an about 20–25 nm wide nanogap into a Au nanowire. The yield of nanogap fabrication is nearly 100% using this technique. The nanoparticles are placed in these 20 nm spaced nanoelectrodes by dielectrophoretic trapping (DEP) applying an AC voltage of 1–2 $V_{\text{peak-peak}}$ at a 1 MHz frequency for 30–50 s. The detailed process is described in [28, 31].

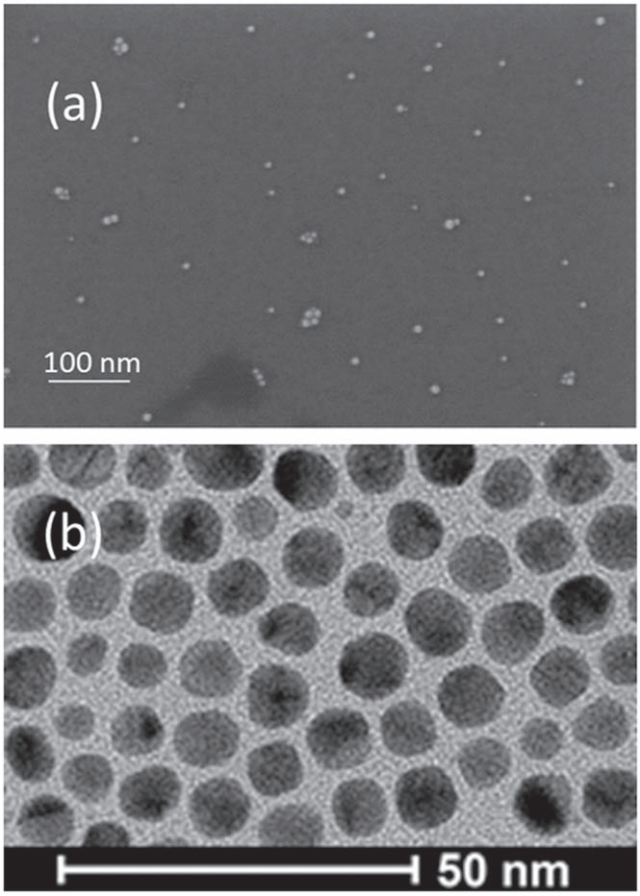

Figure 2. The results of structural analysis of AuNPs, (a), SEM Image of dispersed DDT-AuNPs on the Si surface. In order to obtain nanoparticle agglomerations that show an as close as possible status of AuNPs in solution, a drop of AuNP solution was blow dried on the substrate. (b) TEM image of DDT-AuNPs by drop casting method on the Si TEM Cu grid.

DC Electrical characterization is carried out using an Agilent B1500 in forward and reverse bias by applying DC voltages of up to 500 mV and recording currents flowing through the devices at room temperature.

Molecular functionalization of the thiolate-capped AuNPs with BPDT

For molecular functionalization, the trapped nano-devices were immersed in 5 ml of 10 mmol of biphenyl-4, 4-dithiol solution at room temperature. Argon (Ar) gas was bubbled before immersion of sample to avoid oxidation. The sample is kept in the solution for 48 h while Ar gas continues to flow through the solution.

Results and discussions

The SEM image in figure 2(a) demonstrates that the AuNPs are mono-disperse with few agglomerations containing 2–4 AuNPs. The AuNP size is measured from TEM images for DDT-AuNPs (figure 2(b)). We obtain a DDT-AuNP diameter size d^{TEM} of 7.9 $\pm$ 0.8 nm. For the TEM sample preparation,

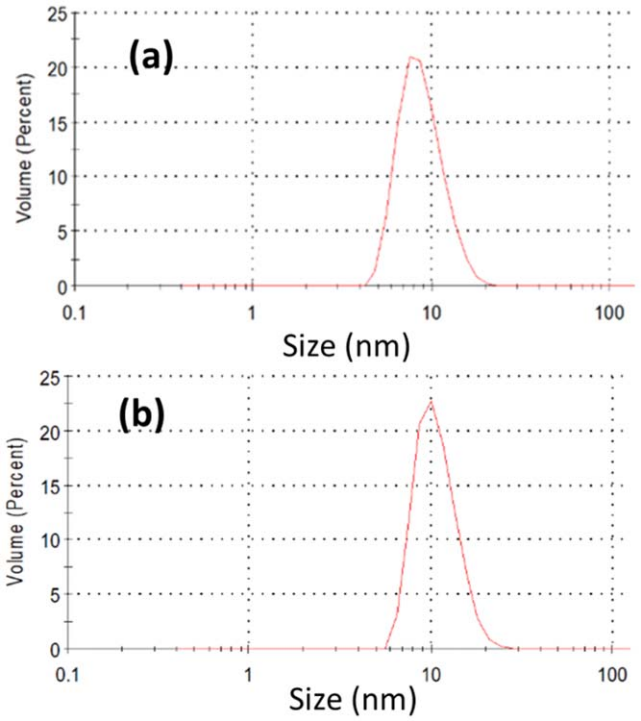

Figure 3. DLS measurement showing hydrodynamic diameter of (a), DDT-AuNPs (b), St-AuNPs.

the solvent is dried slower than for the preparation of the SEM samples. As a consequence, in some places of the TEM grid, AuNP agglomerations are observed, from which the NP–NP spacing is measured. For the DDT-AuNPs, we obtain a NP–NP spacing $d^{\mathrm{NP-NP}}$ of 1.7 ± 0.4 nm (figure 2(b)). It should be noticed that $d^{\mathrm{NP-NP}}$ might be different from the trapped AuNPs in the nanoelectrode gap. Nevertheless, it is likely that during the DEP process, the forces to assemble the NPs are higher than the forces leading to a spontaneous agglomeration on the TEM grid. Therefore, we would expect the $d^{\mathrm{NP-NP}}$ to be smaller in the devices as compared to $d^{\mathrm{NP-NP}}$ on the TEM grid. For the 1-dodecanethiol molecules with a length of about 1.3 nm [32], this means thus that the molecules of neighboured AuNPs are shorter due to conformational changes or interdigitating happens.

From the DLS measurements given in figure 3, we obtain the average hydrodynamic diameter of $d^{\mathrm{DLS}} = 9.5 \pm 1.5$ nm for the DDT-AuNPs and 10.0 ± 1.5 nm for the St-AuNPs. A comparison of d^{TEM} with the d^{DLS} shows that d^{DLS} is 1.7–2.2 nm larger. This difference of d^{TEM} and d^{DLS} is smaller than the double length of the 1-dodecanethiol molecule, which again could indicate, as was already observed in the TEM NP–NP distance measurements, that the molecules in the hydrate shell are binding at oblique angles on the facets of the AuNP surface. These ligand configurations on NPs are given by theoretical simulations, which are showing that the molecules are not completely stretched [31]. Also, it was shown that for molecule densities as are typically present on AuNP surfaces, gauche defects might lead to a further reduction of the length of the ligand shell [33].

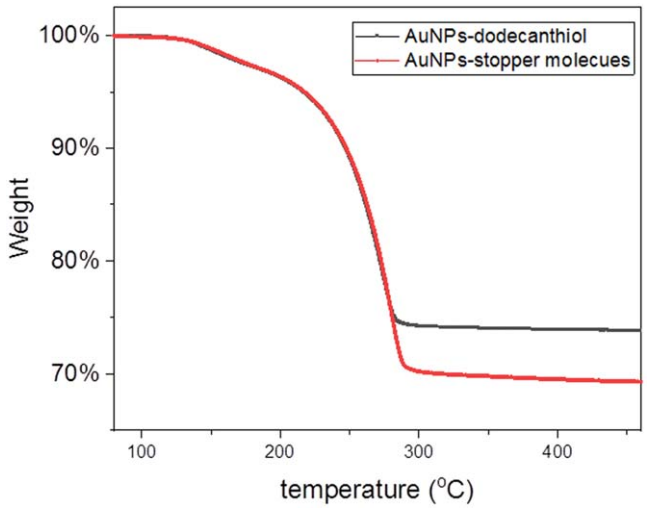

Figure 4. TGA traces for the AuNPs capped with 1-dodecanethiol and stopper molecules.

According to the TGA results given in figure 4, both AuNPs-capped with 1-dodecanethiol and stopper molecules lose weight with the increase of temperature, in three stages: (a) at the $T < 120$ °C stage, there was a slight weight loss that is attributed to the evaporation of the residual solvent; (b) 120 °C $< T <$ 320 °C, an obvious weight loss appeared at this stage, since the ligand molecules on the gold nanoparticles surface decomposed with the continuous heating; (c) $T > 320$ °C, the weight of the samples did not change because all the organic ligands have decomposed and only gold is left. Based on the results, we calculated the weight loss percentage of each sample, which is around 26% for the AuNPs capped with 1-dodecanethiol molecules and 31% for the AuNPs capped with stopper molecules. The weight loss difference comes from the heavier molecular weight of the stopper molecules (733 g mol^{-1}) as compared with the 1-dodecanethiol (179 g mol^{-1}).

Molecule densities were measured on Au (111) surfaces and on AuNP surfaces where the densities of molecules depend on the molecule length and the NP diameter [34–36]. The measured molecule densities are 4–7 molecules nm^{-2} [36]. This corresponds to molecule–molecule distances of 4–5 Å which implies a densely packed molecular film on the AuNP surface. These density values are also reported for the alkane molecules which means, that the AuNPs used in this work contain a dense ligand shell.

After synthesis of the DDT-AuNPs and the St-AuNPs, the nanoMoED devices are fabricated. Such device consists of two nanoelectrodes and at least one nanoparticle bridging the electrode gap. The electrical resistance of such device depends strongly on the NP–NP or NP-electrode distance as well as the nature of the molecules that bridge the gap. The nanoMoED device electrical resistance is thus not only very sensitive to the electrical transmission at the Au-molecule junction, but, it is also related directly to the electronic structure of a single molecule [29]. Therefore, the electrical measurements are a sensitive probe since the device electrical resistance changes with the nature of the AuNP

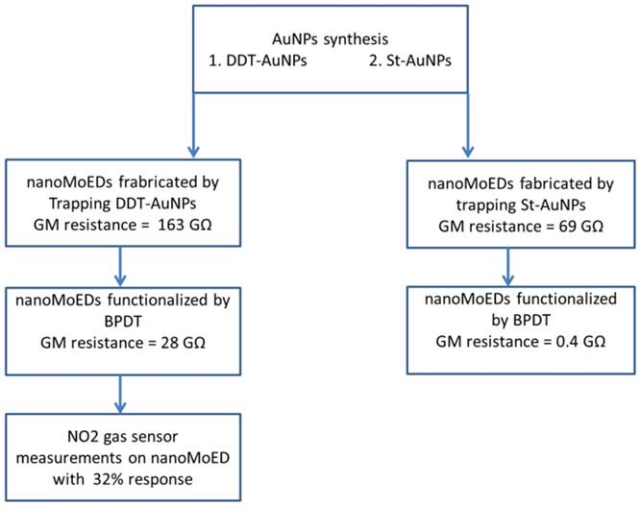

Figure 5. Block diagram summarising this work. After synthesis of DDT- and St-AuNPs, the nanoMoEDs are fabricated by trapping the respective AuNPs in the nanogap. Device electrical resistances are measured both, when trapped with the AuNPs into the nanogaps and after functionalizing of nanoMoED devices with BPDT. The nanoMoED devices containing DDT-AuNPs functionalized with BPDT are used to carry out NO_2 gas sensor measurement.

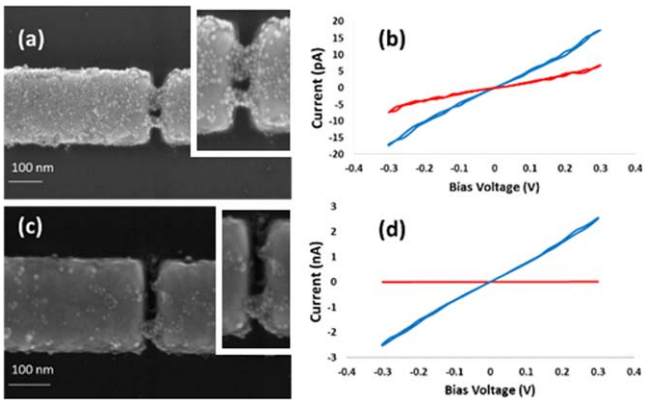

Figure 6. The SEM and electrical characterization of nanoMoED devices, (a), presents SEM image of device trapped with DDT-AuNPs and molecular functionalization with BPDT molecule. (b) *I–V* curves, red curve when device is functionalized with DDT- AuNPs while blue curve presents after functionalization with BPDT. (c) Presents SEM image of device trapped with St-AuNPs and molecular functionalization with BPDT molecule. (d) *I–V* curves, red curve when device is functionalized with St- AuNPs while blue curve presents after functionalization with BPDT. The insets in (a) and (c) show how the AuNPs bridge the nanoelectrode gap.

functionalization shell. Thus, electrical measurements on the nanoMoED device cannot only be used for device applications, but they are also a sensitive tool giving information about the AuNP molecular functionalization shell. The figure 5 summarizes the methodology of this work.

After trapping the AuNPs into the nanoelectrode gap in the nanoMoED, the device electrical resistance was measured. Subsequently, the BPDT molecule is moved into the platform by the ligand functionalization process and the resistance of the same device is measured again. For the DDT-AuNPs based nanoMoED devices, after molecular functionalization with BPDT, the electrical resistance decreases by 1–2 orders of magnitude. But in the case of the nanoMoED devices containing St-AuNPs, the change in resistance value after molecular functionalization is about 2–3 orders. The SEM images of devices fabricated with both types of AuNPs and their corresponding *I–V* curves are given in figure 6. This observation is similar to other ligand functionalization work [22, 23], that has been carried out using different ligand shells around the AuNPs and different molecules for molecular functionalization in nanoMoED devices.

This difference in resistance value is due to the differences in the properties of the surfactant molecules of St- and DDT-AuNPs. The change in device resistance is quantitatively assessed from the resistance histograms of *I–V* measurements taken after DEP trapping of AuNPs and ligand functionalization in figure 7. The geometric mean (GM) resistance of the device histograms of St-AuNPs and DDT-AuNPs is 69 GΩ and 163 GΩ, respectively. The resistances of the devices containing both types of AuNPs are similar confirming that the addition of 5% of stopper molecules to the AuNP functionalization shell did not impact the electrical junctions formed between the NP–NP surfaces. There are several parameters determining the device resistance such as

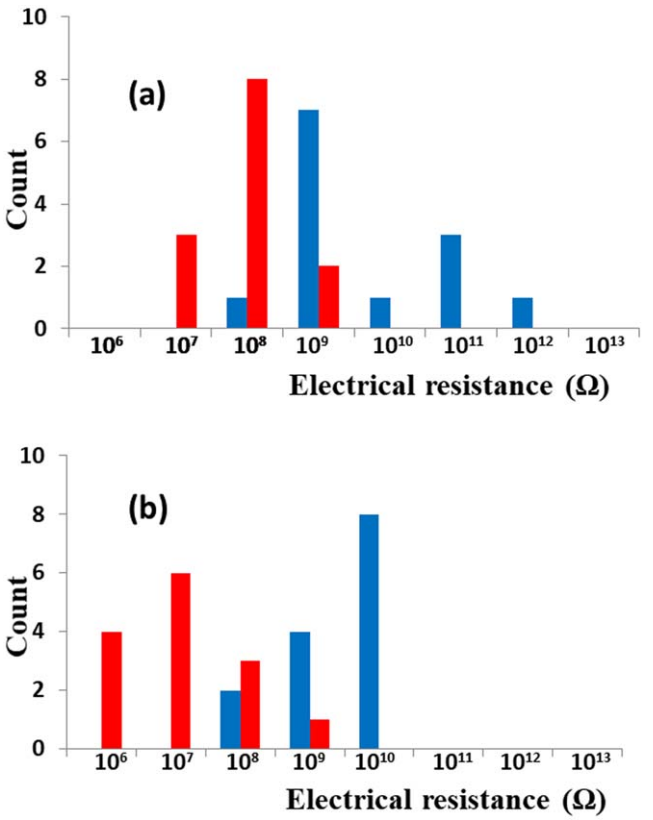

Figure 7. (a) Electrical resistance (Ω) histogram of devices after dielectrophoretic trapping with DDT-AuNPs (blue) and histogram after molecular functionalization with BPDT molecule (red). (b) Resistance (Ω) histogram showing resistance of devices after dielectrophoretic trapping with St-AuNPs (blue) and histogram after molecular functionalization with BPDT molecule (red).

(1) the number of AuNPs forming a conductive bridge between the nanoelectrodes, (2) the type of molecule bridging the gap, (3) the conformation geometry of the molecules bridging the gap [37] as well as (4) the distance between two neighboured Au surfaces. Comparing the St-AuNPs and the DDT-AuNPs, seen that the nanoelectrode spacing is well controlled by the FIB process [19], the number of nanoparticles bridging the gap should be the same, when averaging over a large number of nanoMoED devices as done in the histograms. The TEM measurements of NP–NP spacing indicate that the interparticle spacing in St- and DDT-AuNPs are rather similar. This means that the more bulky stopper molecules, at their concentration of 5%, do not impact the NP–NP spacing. Since the average device resistance for both St- and DDT-AuNPs is similar within the error bar [22], the AuNP distance is not supposed to be responsible for differences in the device resistance. Since the nanoMoED devices low bias electrical resistance does not change significantly when DDT- or St-coated-AuNPs are trapped, we can suppose that the structural differences related to (3) and (4) above do not have a dominant impact on the device resistance, when St- and DDT-AuNPs are compared. In such devices, the tunnel resistance of the device would change drastically with very small changes in the AuNP-AuNP spacing. Thus, the device resistance is very sensitive to changes in the AuNP functionalization shell. Therefore, from the similar resistances of both devices, we conclude that this shell is very similar for both types of nanoMoED device and thus the ligand shell structure that is still dominating AuNP-AuNP spacing is given by the 1-dodecanethiol molecules.

There is a variation in the electrical resistance of devices. In the AuNPs functionalized nanoMoED devices, the ligand shells of neighboured AuNPs will interact through van der Waals bonds. The latter leads to the observed variations of NP–NP spacing which results in the variation of the device resistance. The NP–NP spacing variation is much larger as compared to the spacing of AuNPs that are covalently bound through molecules at both AuNP-molecule junctions [28]. Though this might appear as an inconvenience, it can be an advantage for the molecular functionalization. If the molecules from the primary ligand shell are binding with both ends to neighboured NP with their thiol-endgroups, the NP–NP position would be more rigid, and this leads to less movement in the functionalization shell. This, in turn, might be an additional hinder for the secondary molecule on its way into the primary ligand shell of the AuNPs.

After molecular functionalization with BPDT, the GM resistance in St-AuNPs and DDT-AuNPs based nanoMoED devices decreases to 0.4 GΩ and 28 GΩ, respectively. In a previous work [23], we have shown that AuNPs coated with ω-triphenylmethyl (trityl) protected 1,8-octanedithiol molecules placed in the nanoMoED devices, change of electrical resistance after molecular functionalization is typically 2–3 orders of magnitude. In the DDT-AuNP based devices in this work, we observe a similar 1–2 orders of magnitude change in resistance after molecular functionalization process with BPDT, whereas in St-AuNP based devices, the resistance changes by 2–3 orders of magnitude in the same process. From our analysis, we know that the functionalization shells of the trityl protected 1,8-octanedithiol AuNPs are quite different from the functionalization shell of the DDT- and the St-AuNPs. In the case of the trityl protected 1,8-octanedithiol molecules, we could show in the same publication, that on the surface of these AuNPs, there are both, trityl protected 1,8-octanedithiol and 1,8-octanedithiol molecules in a ratio of 1/3. Furthermore, these 1,8-octanedithiol molecules are lying on the surface, whereas the trityl protected 1,8-octanedithiol molecules are standing on the AuNP surface. This means that a BPDT molecule that approaches such AuNP surface during the molecular functionalization process would encounter many spaces that are not occupied by the bulky trityl protected 1,8-octanedithiol molecules or standing octanedithiol molecules. Thus, the BPDT molecules can get close to the AuNP surfaces. In contrast, when a BPDT molecule approaches the surface of the DDT-AuNP, the BPDT will encounter a surface that is densely packed with 1-dodecanethiol molecules standing on the surface. In turn, in the St-AuNPs, the stopper molecules inserted in the functionalizing 1-dodecanethiol shell, are bulky molecules with an umbrella like endgroup that should locally increase the molecule–molecule spacing on the AuNP surface. This space is used by the BPDT molecules to reach the surface of AuNPs which is a prerequisite for successful molecular functionalization. Since all molecules in these experiments are bound by thiol groups to the Au surface, chemical driving forces favouring the molecular functionalization process can be excluded, and therefore, here, the degree of geometric hindrance is most likely the parameter that determines the rate and degree of molecular functionalization in these devices.

The variation in the final resistance of devices after molecular functionalization is similar to the resistance variation of the trapped AuNPs devices. After molecular functionalization, one more parameter is needed to describe the devices: the position of the BPDT molecules inside the ligand shell. From the TEM measurements, we observe that the interparticle spacing is significantly larger than the BPDT length. This means that one end of the BPDT molecule in the ligand shell is covalently bond to the metal surface while the other end is dangling between the two Au surfaces. We observe that the molecular functionalization process leads to no significant change in the width of the histogram of resistances for both cases, DDT- and St-AuNPs. Thus, the lack of covalent bonds of the BPDT molecule to both sides of the neighboured AuNPs can explain that the electrical resistance histogram did not change significantly.

Thus, the experimental scheme with St-AuNPs and DDT-AuNPs is useful since it allows for a much more simple synthesis of such NPs as compared to the synthesis of NPs in [26] as well as in this scheme, one has the freedom to tune the composition and structure of the functionalisation shell of the AuNPs.

One of the first applications of such a nanoMoED device relying on the functionality of only a few molecules has been the demonstration by its use as a gas sensor [9]. In fact, the nanoMoED device containing DDT-AuNPs and a molecular functionalization with BPDT molecules showed an increase

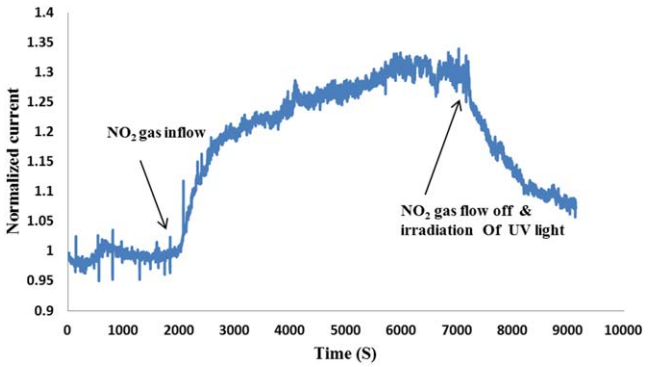

Figure 8. *I–t* measurement on nanoMoED device trapped with DDT-AuNPs and molecular functionalization with BPDT under NO_2 gas environment, *x*-axis presents time in seconds and *y*-axis present normalized current values. When the NO_2 gas flow was stopped, the nanoMoED device was exposed to UV light whereupon the molecular junction resistance increased.

in the electrical current when exposed to NO_2 gas environment, figure 8. This observation is an indication that there is a change of density of states of BPDT molecules in the presence of NO_2 gas [9]. In this reference, we have shown that the Non-equilibrium Green function together with a density function theory calculation on BPDT molecule attached with gold electrodes explains this enhancement of current under NO_2 gas atmosphere being is due to the fact that the BPDT molecular orbitals have a better coupling to the continuum states induced by gold electrodes in the presence of NO_2. The increase of the current upon the exposure of the device to the NO_2 gas is similar to the one measured in [9]. Since alkanethiols have not shown a response to NO_2 gas [9], this result also affirms that the BPDT molecules are present in the nanojunctions and carry a large part of the electrical current in the nanoMoED devices. The measured response to a 13 ppm concentration of NO_2 is 32%.

Conclusion

After having succeeded to insert target molecules via molecular functionalization in nanoMoED devices in Jafri *et al* [23]. We could show that molecular functionalization can equally be reached for a different, but more simplified functionalization shell of NP, where the ligand shell consists of 1-dodecanethiol and 1-dodecanethiol with 5% of stopper molecules. From electrical measurements, we conclude that ligand functionalization leads to devices with a higher electrical transmission for the nanoMoED devices containing the bulky stopper group in St-AuNPs as compared to the ones with DDT-AuNPs. The structural analysis of NPs indicates that the differences in device electrical resistance of St-AuNP based and DDT-AuNP based nanoMoED devices are not related to differences in NP–NP spacing in the two device types. The decrease in device electrical resistance in the presence of the more bulky stopper molecule ligands points to the fact that the decreased steric hindrance in the stopper molecule ligand shell enables more BPDT molecules to move during molecular functionalization into the ligand shell of St-AuNPs leading to an increased electrical transmission of the related devices. Devices built of BPDT functionalized DDT-AuNPs show a similar response as BPDT functionalized AuNPs in [9] to NO_2 in a gas sensing experiment. This shows that the gas sensing principle proposed in that paper is valid also for BPDT incorporated into different ligand shells and this observation is therefore an important step to demonstrate the universality of this single and few molecules-based gas sensor principle, where the device response corresponds to the response of single molecule.

Acknowledgments

We are grateful to the support of this work from Swedish Science Council grant 2106-05259, Knut and Alice Wallenberg Foundation 2011.0082, Formas 2019-01538, Aforsk 20-280, Olle Engkvist 211-0068, Qilu Young Scholar Program of Shandong University, and Shandong Natural Science Foundation of China (Grant No.: ZR2021QE148). We are thankful to Mirpur University of Science and Technology (MUST), Pakistan for financing Omer Sher studies. The financial support from the Swedish Research Council (VR-2016-06014).

Data availability statement

The data generated and/or analysed during the current study are not publicly available for legal/ethical reasons but are available from the corresponding author on reasonable request.

ORCID iDs

Omer Sher https://orcid.org/0000-0001-5344-6768
Anton Grigoriev https://orcid.org/0000-0001-5389-2469
Klaus Leifer https://orcid.org/0000-0002-8360-1877

References

[1] Huang C, Rudnev A V, Hong W and Wandlowski T 2015 *Chem. Soc. Rev.* **44** 889–901
[2] Xiang D, Jeong H, Lee T and Mayer D 2013 *Adv. Mater.* **25** 4845–67
[3] Schwarz F and Lörtscher E 2014 *J. Phys.:Condens. Matter.* **26** 474201
[4] Prokopuk N and Son K A 2008 *J. Phys.:Condens. Matter.* **20** 374116
[5] Metzger R M 2015 *Chem. Rev.* **115** 5056–115
[6] Yin X, Zang Y, Zhu L, Low J Z, Liu Z F, Cui J, Neaton J B, Venkataraman L and Campos L M 2017 *Sci. Adv.* **3** eaao2615
[7] Chen Y, Xianyu Y and Jiang X 2017 *Acc. Chem. Res.* **50** 310–9
[8] Xin N, Guan J, Zhou C, Chen X, Gu C, Li Y, Ratner M A, Nitzan A, Stoddart J F and Guo X 2019 *Nat. Rev. Phys.* **1** 211–30
[9] Wani I H *et al* 2019 *Nanoscale Commun.: Nanoscale* **11** 6571
[10] Song H, Kim Y, Jang Y H, Jeong H, Reed M A and Lee T 2009 *Nature* **462** 1039–43

[11] Sun L, Diaz-Fernandez Y A, Gschneidtner T A, Westerlund F, Lara-Avila S and Moth-Poulsen K 2014 *Chem. Soc. Rev.* **43** 7378–411
[12] Xiang D, Wang X, Jia C, Lee T and Guo X 2016 *Chem. Rev.* **116** 4318–440
[13] Vilan A and Cahen D 2010 *AIP Conf. Proc.* **1313** 30–3
[14] Jafri S H M, Blom T, Wallner A, Ottosson H and Leifer K 2014 *J. Nanopart. Res.* **16** 2811
[15] Mathew P T and Fang F 2018 *Engineering* **4** 760–71
[16] Dadosh T, Gordin Y, Krahne R, Khivrich I, Mahalu D, Frydman V, Sperling J, Yacoby A and Bar-Joseph I 2005 *Nature* **436** 677–80
[17] Hadeed F O and Durkan C 2007 *Appl. Phys. Lett.* **91** 123120
[18] Jeong H, Kim D, Xiang D and Lee T 2017 *ACS Nano* **11** 6511–48
[19] Blom T, Welch K, Strømme M, Coronel E and Leifer K 2007 *Nanotechnology* **18** 285301
[20] Li H, Wani I H, Hayat A, Jafri S H M and Leifer K 2015 *Appl. Phys. Lett.* **107** 103108
[21] Smith A M, Marbella L E, Johnston K A, Hartmann M J, Crawford S E, Kozycz L M, Seferos D S and Millstone J E 2015 *Anal. Chem.* **87** 2771–8
[22] Calard F, Wani I H, Hayat A, Jarrosson T, Lère-Porte J-P, Jafri S H M, Serein-Spirau F, Leifer K and Orthaber A 2017 *Mol. Syst. Des. Eng.* **2** 133–9
[23] Jafri S H M, Hayat A, Wallner A, Sher O, Orthaber A, Ottosson H and Leifer K 2020 *Nanotechnology* **31** 225207
[24] Ratner M 2013 *Nat. Nanotechnol.* **8** 378–81
[25] Lörtscher E 2013 *Nat. Nanotechnol.* **8** 381–4
[26] Wallner A, Jafri S H M, Blom T, Gogoll A, Leifer K, Baumgartner J and Ottosson H 2011 *Langmuir* **27** 9057–67
[27] Sugunan A, Jafri S H M, Qin J, Blom T, Toprak M S, Leifer K and Muhammed M 2010 *J. Mater. Chem.* **20** 1208–14
[28] Jafri S H M, Löfås H, Blom T, Wallner A, Grigoriev A, Ahuja R, Ottosson H and Leifer K 2015 *Sci. Rep.* **5** 1–11
[29] Jafri S H M, Löfås H, Fransson J, Blom T, Grigoriev A, Wallner A, Ahuja R, Ottosson H and Leifer K 2013 *Nanoscale* **5** 4673–7
[30] Sugie A, Somete T, Kanie K, Muramatsu A and Mori A 2008 *Chem. Commun.* 3882–4
[31] Jafri S H M, Blom T, Leifer K, Strømme M, Löfås H, Grigoriev A, Ahuja R and Welch K 2010 *Nanotechnology* **21** 435204
[32] Zabet-Khosousi A and Dhirani A A 2008 *Chem. Rev.* **108** 4072–124
[33] Devi J M 2017 *J. Mol. Graph. Modell.* **74** 359–65
[34] Hill H D, Millstone J E, Banholzer M J and Mirkin C A 2008 *Bone* **23** 1–7
[35] Lanterna A E, Coronado E A and Granados A M 2012 *J. Phys. Chem.* C **116** 6520–9
[36] Hinterwirth H, Kappel S, Waitz T, Prohaska T, Lindner W and Lämmerhofer M 2013 *ACS Nano* **7** 1129–36
[37] Mishchenko A *et al* 2010 *Nano Lett.* **10** 156–63